J Incl Phenom Macrocycl Chem (2011) 70:461–469
DOI 10.1007/s10847-010-9897-y

ORIGINAL ARTICLE

# Inclusion complex of α-cyclodextrin and the extended viologen dication: a model of an insulated molecular wire

**Magdaléna Hromadová · Viliam Kolivoška · Miroslav Gál · Lubomír Pospíšil · Romana Sokolová · Michal Valášek**

Received: 2 July 2010 / Accepted: 24 October 2010 / Published online: 17 November 2010


**Abstract** An extended viologen dication **1**, containing one viologen subunit, was used as a model for the inclusion complex formation between cyclodextrin (CD) molecules and molecular wires comprising several subunits. UV–Vis and fluorescence spectroscopic measurements confirmed the formation of two types of the inclusion complexes 1:1 and 2:1 between αCD and **1** in the aqueous solution containing 20% of ethanol. The complex formation constants were obtained from the fluorescence spectral changes: $K_a = 25 \pm 3\ \mathrm{mM}^{-1}$ for [αCD–**1**] complex and $K_a = 0.21 \pm 0.07\ \mathrm{mM}^{-2}$ for [$(\alpha\mathrm{CD})_2$–**1**] complex, respectively. Cyclodextrins βCD and γCD do not form the inclusion complexes with **1** in these aqueous solutions. The time-dependent differential capacitance measurements confirmed the adsorption of **1** in the form of a complex at the electrode/electrolyte interface. These studies were conducted with the aim to find the most suitable CD cavity that would separate individual molecular wires from each other on the electrode/electrolyte interface.

**Keywords** α-Cyclodextrin · Extended viologen · Complex formation · Ac voltammetry

M. Hromadová (✉) · V. Kolivoška · M. Gál · L. Pospíšil · R. Sokolová
J. Heyrovský Institute of Physical Chemistry of ASCR, v.v.i., Academy of Sciences of the Czech Republic, Dolejškova 3, 18223 Prague, Czech Republic
e-mail: hromadom@jh-inst.cas.cz

M. Valášek
Institute of Organic Chemistry and Biochemistry ASCR, v.v.i., Academy of Sciences of the Czech Republic, Flemingovo n. 2, 16610 Prague, Czech Republic

## Introduction

Cyclodextrins are oligosaccharides, which consist of six (α-cyclodextrin), seven (β-cyclodextrin), eight (γ-cyclodextrin) or more glucopyranose units linked through the α(1–4) glycosidic bonds into a doughnut shaped ring. The internal cavity diameter of these compounds is reported in the range 0.47–0.53 nm for α-cyclodextrin (αCD), 0.60–0.65 nm for β-cyclodextrin (βCD), and 0.75–0.83 nm for γ-cyclodextrin (γCD), respectively [1, 2]. The ability of cyclodextrins to act as molecular hosts has been demonstrated in many areas of everyday life: in the chemical analysis and chiral separations, cosmetics, pharmacology, environmental and food industries [3, 4].

Extended viologens represent a group of organic molecules that are intended to be used as molecular wires in the molecular electronic devices [5–7]. Recently, a possibility to alter the electric properties of molecular wires by coating them with cyclodextrin molecules was demonstrated by quantum mechanical calculations [8], electroluminescence [9, 10] and electric conductivity measurements [11]. The individual insulated molecular wires can be formed for example from a conducting polyaniline polymer and the molecular nanotube synthesized from individual αCD molecules [12]. It was shown recently that the chemical oxidation of the polyaniline backbone by the iodine molecules can be completely blocked in the presence of αCD [13].

The formation of the host–guest complexes of cyclodextrins with many types of the organic, inorganic and organometallic compounds is detected mainly by various spectroscopic methods based on the changes of spectra upon complexation [14–17]. An application of electrochemical techniques to the detection of the inclusion complexes is much less common since several

requirements should be fulfilled. A studied compound should be electroactive and the system must contain high concentration of the supporting electrolyte. Therefore, the values of the complex formation constants obtained by the electrochemical methods are reported at high ionic strengths. Only recently a use of the ultramicroelectrodes permitted the determination of the complex formation constants in the systems without supporting electrolyte [18]. The electrochemical measurements can prove the formation of cyclodextrin complexes either from a decrease of the diffusion-limited currents resulting from a change of the diffusion coefficient or as a rather subtle shift of the redox potential [19–21]. The latter effect is a safe criterion for the reversible redox systems [22], whereas the irreversible electron transfer reactions may bring complications due to the coupling of electron transfer kinetics to the subsequent chemical steps or due to the influence of the adsorptive inhibition of cyclodextrins accumulated at the electrode surface [23, 24]. One important advantage of the electrochemical techniques over the spectroscopic ones is the possibility to obtain in addition to the complex formation constants also the formation and dissociation rate constants of the inclusion complexes by the numerical simulation methods [19, 25]. In this work we studied the changes in the structure of the electrode/electrolyte interface in the double-layer region and the changes in the apparent diffusion coefficient of **1** to assess the complex formation ability of **1** with cyclodextrins as well as the ability of the complexes to adsorb at the electrode surface. This procedure turned out to be particularly useful for systems with small values of the complex formation constants.

Data on the complex formation ability of the extended viologen molecules, i.e. those that have some spacer between two pyridinium moieties are virtually not existent to the best of our knowledge. There is only one report on the complex formation between tetramethylene bis-4 (1-benzylpyridine-4′-yl)pyridinium and βCD [26], whereas the inclusion complexes have been confirmed for many viologens, i.e. 1,1′-disubstituted-4,4′-bipyridinium compounds [27–34]. Kitamura et al. [29] confirmed that both αCD and βCD associate with viologens in the bulk of the aqueous solution, whereas viologens with the alkyl chains longer than butyl form also the surface-confined inclusion complexes with αCD. Once the viologen moiety is reduced to the cation radical state αCD is released from the surface into the solution. Complex formation affects also the dimerization of such viologen cation radicals. The dimerization of dibutylviologen cation radicals in the presence of αCD is almost completely suppressed due to a steric hindrance [30], which holds also for viologens with longer alkyl chains. In order to weaken the intermolecular interactions of n-heptylviologen molecules in the electrochromic displays Yasuda et al. [26] formed their inclusion complexes with βCD. The authors also concluded that the complex formation inhibits the dimerization process and the inclusion site depends on the redox state of viologen. This work also brings a report on the complex formation between extended viologen tetramethylene bis-4(1-benzylpyridine-4′-yl)pyridinium and βCD for comparison with n-heptylviologen behavior. The authors state that the former compound forms stronger complexes by phenyl ring incorporation inside the βCD cavity. Electroactive self-assembled monolayers of the simple viologens have been prepared on the gold electrodes by Yan et al. [35], who also confirmed the formation of the surface-confined inclusion complexes with cyclodextrin molecules.

The main objective of this work is to study the complex formation ability of a short molecular wire based on the extended viologen (Scheme 1) with cyclodextrin molecules of different cavity sizes (αCD, βCD and γCD). Work presented in this paper is a prerequisite for studies of the electron transfer properties of the extended viologen molecules (molecular wires) in their free form and in their complexes with cyclodextrins.

## Experimental

Compound 1,4-bis[4-(4-methylsulfanylphenyl)-2,6-diphenylpyridinium-1-yl]benzene triflate (**1**) was synthesized by Valášek et al. [36] according to the general procedure described elsewhere. Desired product **1** was prepared in 89% yield: $^{1}$H NMR (400 MHz, $d_6$-DMSO) δ ppm: 2.57 (s, 6H, –SMe), 7.20–7.28 (m, 16H, Ar), 7.43 (d, J = 8.8 Hz, 4H, MeSAr), 7.49–7.55 (m, 8H, Ar), 8.26 (d, J = 8.8 Hz, 4H, MeSAr), 8.41 (s, 4H, pyrid.). $^{13}$C NMR (100 MHz, $d_6$-DMSO) δ ppm: 13.87 (–SMe), 124.50, 125.83, 128.42, 128.88, 129.19, 129.26, 130.83, 132.37, 140.11, 145.90, 154.37, 156.14. IR (KBr pellet) $\nu$ cm$^{-1}$ 3100 and 3061 (bw, $\nu$(CH), pyrid. and arom.), 1619 and 1588 (s, $\nu$(C–C), pyrid. and arom.), 1496 (m, $\nu$(C–C), arom.), 1265 (bs, $\nu_{as}(SO_3^-)$), 1154 (bm, $\nu(CF_3)$), 1029 (m, $\nu_s(SO_3^-)$), 832 a 819 (w,

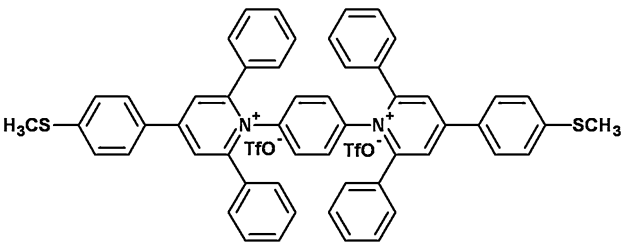


**1**

**Scheme 1** Chemical structure of 1,4-bis[4-(4-methylsulfanylphenyl)-2,6-diphenylpyridinium-1-yl] benzene triflate

γ(CH), Phe), 759 and 699 (m, γ(CH), Ph), 637 (m, $\delta_s(CF_3)$). ESI MS *m/z* (%) 391.5 (100, $[M\text{-}2A]^{2+}$). Anal. calcd. for $C_{56}H_{42}F_6N_2O_6S_4$ (1081.20): C, 62.21; H, 3.92; N, 2.59. Found: C, 62.32; H, 3.98; N, 2.65.

NMR spectra were recorded with a Varian INOVA-400 and Bruker Avance 400 spectrometer at 25 °C in $d_6$-DMSO. $^1$H NMR (400 MHz) spectra were referenced to TMS as internal standard ($\delta_H = 0$ ppm). $^{13}$C NMR (100.58 MHz) spectra with total decoupling of protons was referenced to signal of the solvent ($d_6$-DMSO, $\delta_C = 39.52$ ppm). ESI MS spectra were recorded with a Bruker Esquire 3000 spectrometer (sample was dissolved in MeOH). IR spectra were recorded with a Bruker EQUINOX 55 (IFS 55) spectrometer as KBr pellets. Analytical samples were dried at 100–120 °C under reduced pressure (1.4 Pa). Elemental analyses were obtained using a Perkin-Elmer 2400 Series II analyser.

Deionized water with a maximum resistivity of 18 MΩ cm was obtained by means of a Milli-Q RG purification system, Millipore Co., USA and was used throughout the studies. Ethanol, p.a. (Lach-Ner, Czech Republic) and potassium fluoride, p.a. (Merck, Germany) were used as received. All three cyclodextrins were of the best quality available from Sigma (αCD, γCD) and Fluka (βCD).

The electrochemical measurements were made using a laboratory-built electrochemical system consisting of a fast rise-time potentiostat and a lock-in amplifier (Stanford Research, model SR830). The instruments were interfaced to a personal computer via an IEEE-interface card (PC-Lab, AdvanTech Model PCL-848) and a data acquisition card (PCL-818) using 12-bit precision. A three-electrode electrochemical cell was used. The reference electrode (Ag|AgCl|1 M LiCl) was separated from the test solution by a salt bridge with a double fritted junction. A valve-operated static mercury drop electrode SMDE2 (Laboratorní Přístroje, Prague) of area 0.0155 cm$^2$ was used as a working electrode. Platinum net was used as the auxiliary electrode. Oxygen was removed from the solution by a stream of argon. A protecting argon layer blanketed the solution surface during the entire experiment.

UV–Vis spectra were obtained either using Perkin-Elmer UV/Vis/NIR spectrometer Lambda 1050 (Perkin-Elmer, USA) or using a diode-array UV–Vis spectrometer Agilent 8453. The fluorescence emission spectra were recorded using a Perkin-Elmer luminescence spectrometer model LS 50B (Perkin-Elmer, USA) at the excitation wavelength of 379 nm. The excitation and emission bandwidth was set to 5 nm. A quartz cuvette with an optical path of 1 cm was used in both cases. The stock solution of **1** was prepared in 20% ethanol/water mixture (v/v), which was later divided into two parts. The solid cyclodextrin compound was added to the second part to get the maximum concentration of CD to be measured. These two solutions were then mixed in different v/v ratios to obtain the measured solutions. The same procedure was followed for the preparation of the blank solutions except instead of the stock solution of **1** only the 20% ethanol/water mixture was used. The absorption and emission spectra of 20% ethanol/water mixture in the absence and presence of different concentrations of cyclodextrin molecules were used as blanks for the correction of all the reported spectral measurements.

## Results and discussion

Due to a limited solubility of the wire **1** in pure water the complex formation ability of **1** with cyclodextrin (CD) molecules of different cavity sizes (αCD, βCD and γCD) was studied in 20% ethanol/water mixture. Figure 1 shows a comparison of two data sets of UV–Vis absorption spectra of **1** after an addition of either αCD or βCD, respectively. The data for γCD additions are not shown, but are qualitatively the same as those for βCD. The extinction coefficient of the absorption band at $\lambda_{max} = 392$ nm in the absence of cyclodextrins is 67,800 ± 1,500 $M^{-1}$ $cm^{-1}$ (data not shown) and originates from the π–π* transition(s) of the conjugated phenylpyridinium backbone of the extended viologen **1**. For comparison, a very similar compound containing 1,4-phenylene-bis-4,4′-pyridinium moiety exhibits a broad intense absorption band with a maximum near 335 nm, which has been reported to originate from three π–π* transitions of the aromatic backbone [6]. From Fig. 1 it is immediately discernible, that the UV–Vis spectra show significant changes only in the presence of αCD molecules. There is no shift in the position of the absorption maximum, whereas the absorbance values increase with increasing concentration of αCD exhibiting an increase in the extinction coefficient of **1** in the presence of αCD. Only a slight almost insignificant increase of the absorbance was observed for βCD and γCD additions.

The data from Fig. 1 were subjected to Benesi–Hildebrand (BH) analysis [37–39] at the wavelength of the maximum absorbance ($\lambda_{max} = 392$ nm), which enables the determination of the complex stoichiometry. The Benesi–Hildebrand equation for a 1:1 inclusion complex formation, assuming the excess of CD concentration with respect to **1**, can be expressed as

$$\frac{1}{\Delta A} = \frac{1}{\Delta\varepsilon[G]} + \frac{1}{\Delta\varepsilon[G]K_a} \cdot \frac{1}{[CD]} \quad (1)$$

where [G] and [CD] are the analytical concentrations of the guest G and host CD molecules, $\Delta A = A - A_0$ is the change in the absorbance after CD addition, $A_0$ and $A$ are the absorbances of **1** in the absence and presence of CD, $\Delta\varepsilon$ is the difference in the molar absorptivities between the complexed and free guest. The complex formation constant

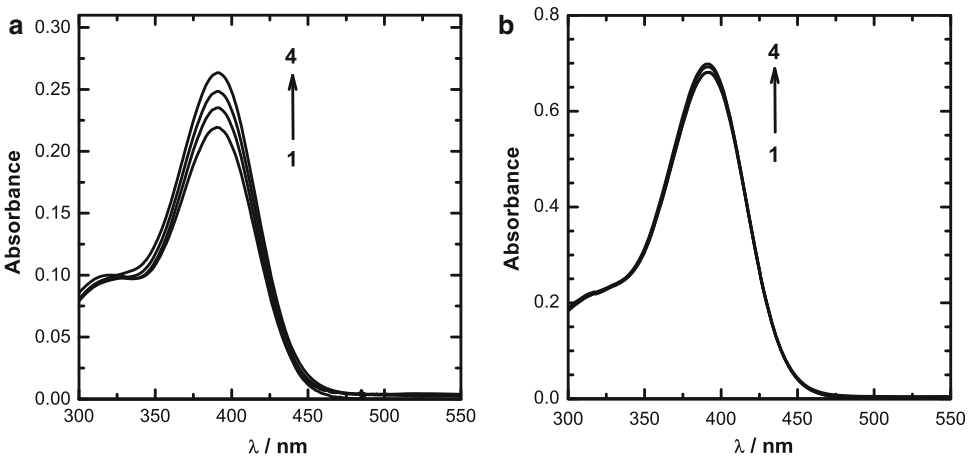


**Fig. 1** **a** UV–Vis absorption spectra of $5 \times 10^{-6}$ M wire **1** in 20% ethanol/water solvent in the presence of 0 M (1), $2 \times 10^{-4}$ M (2), $1.2 \times 10^{-3}$ M (3) and $2 \times 10^{-3}$ M (4) αCD. **b** UV–Vis absorption spectra of $1 \times 10^{-5}$ M wire **1** in 20% ethanol/water solvent in the presence of 0 M (1), $1.2 \times 10^{-3}$ M (2), $3.3 \times 10^{-3}$ M (3) and $5.5 \times 10^{-3}$ M (4) βCD

$K_a$ is obtained from the intercept/slope ratio. If a 2:1 inclusion complex is formed the Benesi–Hildebrand equation, assuming the excess of CD concentration with respect to **1**, takes on the form

$$\frac{1}{\Delta A} = \frac{1}{\Delta\varepsilon[\mathrm{G}]} + \frac{1}{\Delta\varepsilon[\mathrm{G}]K_a} \cdot \frac{1}{[\mathrm{CD}]^2} \qquad (2)$$

where the symbols have the same meaning as in the Eq. 1. The complex formation constant $K_a$ is obtained from the intercept/slope ratio. The results of the BH analyses are shown in Fig. 2. The expected linearity of the Benesi–Hildebrand plot is observed neither for the double reciprocal plot of $1/\Delta A$ against the 1/[αCD] nor for $1/\Delta A$ against the $1/[\alpha\mathrm{CD}]^2$.

This finding points to the fact that the solution most likely contains both types of the complexes: 1:1 as well as 2:1 complex, respectively. The space filling model obtained by Spartan'08 program (Wavefunction, Inc., USA) confirms such a possibility (see Fig. 3). It indicates that the phenyl groups located in the 2 and 6 positions on the pyridinium moieties are too close to each other to allow for their inclusion into the αCD cavities and so only two possibilities for the inclusion complex formation remain. These are the two equivalent 4-methylsulfanylphenyl fragments on the opposite sides of the molecule. Figure 3 shows the space filling model of the 1:1 complex.

The space filling model in Fig. 3 also suggests a possibility for the 2:1 complex formation by an inclusion of the second 4-methylsulfanylphenyl fragment. It was shown

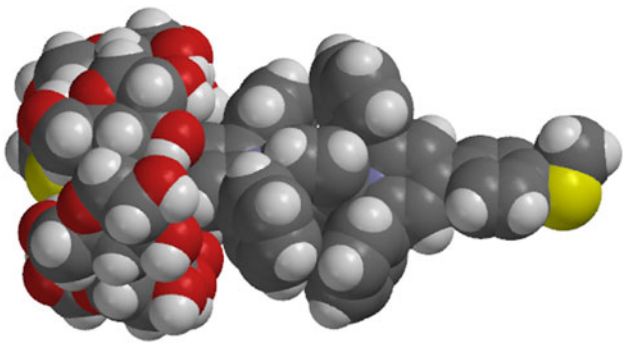

**Fig. 3** Space-filling molecular model of the [αCD–**1**] complex (*grey* carbon, *white* hydrogen, *red* oxygen, *blue* nitrogen and *yellow* sulfur) obtained by Spartan'08

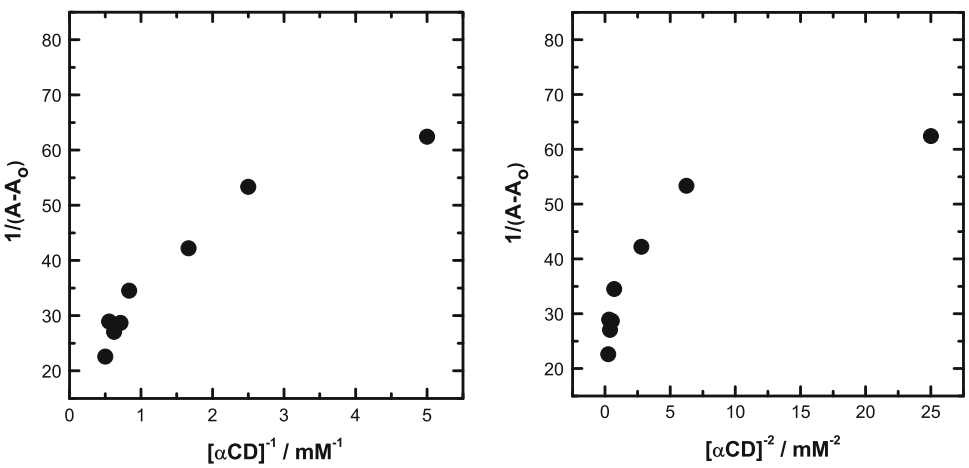


**Fig. 2** Benesi–Hildebrand analysis of the complex formation between **1** and αCD assuming either 1:1 (left panel) or 1:2 (right panel) stoichiometry. The absorbance was obtained at $\lambda_{max} = 392$ nm from the absorption spectra in Fig. 1a. All concentrations are in mM units

recently that the fluorescence spectroscopy is a useful method for studies of the stepwise formation of the 2:1 complexes [16]. Therefore, the complex formation equilibria were studied by the fluorescence spectroscopic technique. Figure 4 shows the fluorescence emission spectra of wire **1** in 20% ethanol/water mixture upon the αCD addition. An excitation wavelength for the measurement of the emission spectra was fixed at $\lambda_{ex} = 379$ nm. A notable increase in the fluorescence intensity of **1** was observed with increasing concentration of αCD confirming the complex formation. The data in the inset of Fig. 4 represent the integrated fluorescence intensity (integrated *FI*) as a function of the increasing αCD concentration. The integrated *FI* values reach a plateau at the concentration ratio of αCD to **1** equal to approximately 100. The presence of such a plateau is a strong indication that at first the 1:1 complex is formed, whereas at sufficiently high concentrations of cyclodextrin the 2:1 complexes prevail in the system [16]. This hypothesis was checked by the construction of the BH double reciprocal plots corresponding to either the formation of 1:1 or 2:1 complexes. The data are shown in Fig. 5.

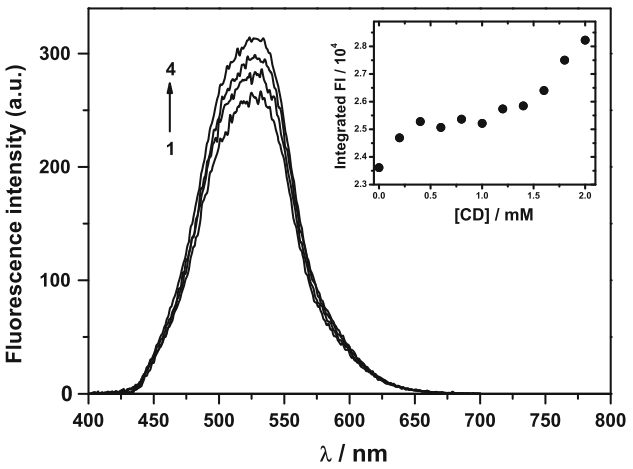


**Fig. 4** Fluorescence emission spectra of $5 \times 10^{-6}$ M wire **1** in the absence (1) and presence of $0.8 \times 10^{-3}$ M (2), $1.6 \times 10^{-3}$ M (3) and $2 \times 10^{-3}$ M (4) αCD in 20% ethanol/water solvent. The *inset* shows integrated fluorescence intensity as a function of the αCD concentration

If the host–guest complex has a stoichiometry 1:1 then the Benesi–Hildebrand equation for the fluorescence intensity change is written as [14, 16]

$$\frac{1}{F - F_0} = \frac{1}{(F_\infty - F_0)K_a[\mathrm{CD}]} + \frac{1}{F_\infty - F_0} \tag{3}$$

If the stoichiometry is 2:1 then the following equation applies

$$\frac{1}{F - F_0} = \frac{1}{(F_\infty - F_0)K_a[\mathrm{CD}]^2} + \frac{1}{F_\infty - F_0} \tag{4}$$

In both equations $F$ is the observed fluorescence intensity at the selected emission wavelength, $F_0$ is the fluorescence intensity of **1** in the absence of αCD, $F_\infty$ is the fluorescence intensity, when all of the wire **1** molecules are in the form of an inclusion complex, and [CD] is for all practical purposes the analytical concentration of αCD. With the help of the inset in Fig. 4 one can immediately recognize that the formation of the complexes between αCD and **1** proceeds in a stepwise manner. Only the first few data points in the left panel of Fig. 5 can be used for BH analysis expressed by Eq. 3, i.e. the formation of the 1:1 complex (the concentration ratio of αCD to **1** not exceeding 100). The rest of the data is not suitable for this type of analysis. Even though one can recognize two linear segments in the data (see the left panel in Fig. 5) the other linear segment would lead to meaningless parameters, since the intercept will reach a negative value (see Eq. 3). On the other hand, the double reciprocal plot of $1/(F - F_0)$ against $1/[\mathrm{CD}]^2$ clearly indicates in this αCD concentration range a good linearity and positive intercept (see the right panel in Fig. 5). From the linear segments in Fig. 5 the following values of the complex formation constants were obtained: for the [αCD–**1**] complex $K_a = [\alpha\mathrm{CD}\text{–}\mathbf{1}]/[\alpha\mathrm{CD}]\,[\mathbf{1}] = 25 \pm 3\ \mathrm{mM}^{-1}$ and for the [$(\alpha\mathrm{CD})_2$–**1**] complex $K_a = [(\alpha\mathrm{CD})_2\text{–}\mathbf{1}]/[\alpha\mathrm{CD}]^2[\mathbf{1}] =$

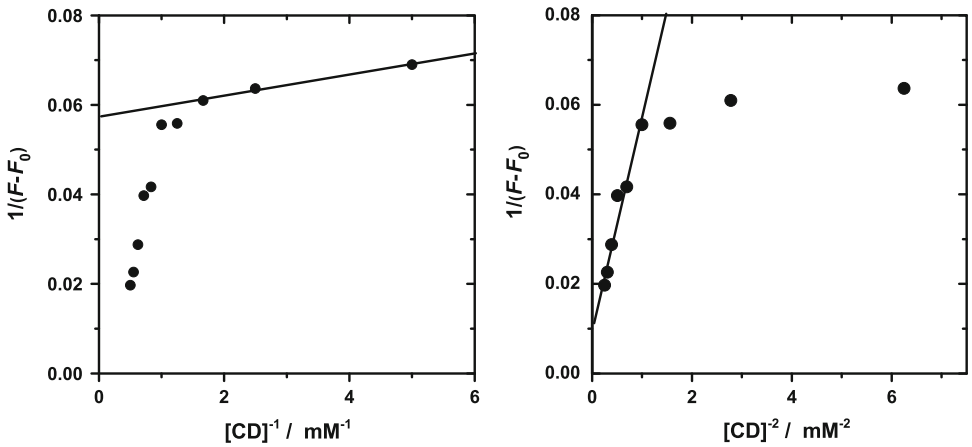


**Fig. 5** Double reciprocal plot of $1/(F - F_0)$ against $1/[\mathrm{CD}]$ (*left panel*) and $1/(F - F_0)$ against $1/[\mathrm{CD}]^2$ (*right panel*) constructed at $\lambda_{em} = 525$ nm from the fluorescence data in Fig. 4

$0.21 \pm 0.07$ mM$^{-2}$, respectively. Assuming $K_a = 20$ mM$^{-1}$ for the [αCD–**1**] complex formation one can easily calculate that at 5 μM concentration of the wire **1** and at 0.5 mM concentration of αCD 99.8% of the wire **1** is in its complexed form [αCD–**1**]. The use of the expressions that would simultaneously consider both 1:1 and 2:1 equilibria was not attempted due to the limited number of data points.

The complex formation ability of **1** with αCD was independently confirmed by the electrochemical AC voltammetric measurements at frequency $f = 160$ Hz. The measured value of the out-of-phase admittance $Y''$ is related to the differential capacitance $C = Y''/(2\pi f)$ of the electrode/electrolyte interface, which in turn provides information on the structure of the electrode/electrolyte interface. Figure 6 shows the $Y''$ admittance of the supporting electrolyte in the absence (empty squares) and the presence of $1.2 \times 10^{-3}$ M αCD (filled squares). The $Y''$ admittance values coincide at the potentials more negative than −0.6 V confirming no αCD adsorption at these electrode potentials. The admittance decreases in the potential range between −0.3 and −0.52 V and reaches a constant value independent of the αCD concentration, which confirms that αCD adsorbs at these potentials in a form of a compact monolayer. Comparison of the same quantities for the supporting electrolyte in the absence (empty squares) and the presence of $5 \times 10^{-6}$ M wire **1** (filled circles) indicates also a compact film formation of wire **1** in the potential range −0.3 to −0.65 V. The capacitance values are higher than those for αCD adsorption. At more negative potentials the onset of the reduction of **1** in the adsorbed state is indicated by a faradaic contribution to both $Y'$ and $Y''$ components (see peaks at −0.77 and −0.95 V in Fig. 6).

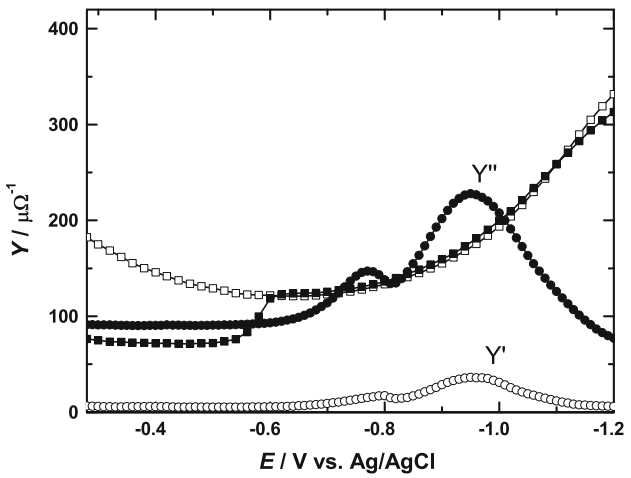


**Fig. 6** AC voltammogram of 0.1 M KF in 20% ethanol/water solvent in the absence (*open squares*) and presence of $1.2 \times 10^{-3}$ M αCD (*filled squares*) or $5 \times 10^{-6}$ M wire **1** (*filled circles*) obtained on HMDE using frequency 160 Hz and amplitude 5 mV. *Filled* and *empty circles* correspond to the out-of-phase ($Y''$) and in-phase ($Y'$) admittances of $5 \times 10^{-6}$ M wire **1**, respectively

Our objective for the future work is to form a compact film of the [αCD–**1**] complex on the electrode surface. Hence, we studied the kinetics of the film formation of **1** in the potential region, where neither adsorption of αCD nor the reduction of **1** is observed, whereas the adsorption of **1** is confirmed by the admittance measurements. These conditions are fulfilled for the electrode potential −0.6 V, which was used in further studies. The experiments were adjusted in such a way that the adsorption of **1** follows the diffusion-limited adsorption and the differential capacitance–time transients can be described by the Koryta equation [40]

$$\zeta = \frac{\pi}{4\mathrm{D}} \cdot \frac{\Gamma^2}{c^2} \tag{5}$$

where $\zeta$ is the characteristic time of the film formation, D is the diffusion coefficient of **1**, $c$ is the concentration of wire **1** in the bulk and $\Gamma$ is the surface concentration of **1** in the units of mol/cm$^2$. It is convenient to transform the experimentally observed out-of-phase admittance–time transients ($Y'' - t$) to the corresponding differential capacitance–time transients ($C - t$). From the capacitance values one can calculate the surface coverage $\theta$ as a function of time using the following equation

$$\theta(t) = \frac{C(t) - C_0}{C_\infty - C_0} \tag{6}$$

where $C(t)$ is the differential capacitance at time $t$, $C_o$ is the differential capacitance of the supporting electrolyte and $C_\infty$ is the differential capacitance at t→ ∞ corresponding to the capacitance of the full surface coverage of the adsorbed species.

The dependence of the surface coverage $\theta$ on time is shown in Fig. 7 for $5 \times 10^{-6}$ M wire **1** (empty circles). Time, at which the surface coverage reaches $\theta = 1$ is the characteristic time $\zeta$ of the film formation. For the solution containing $5 \times 10^{-6}$ M wire **1** we obtained $\zeta = 43$ s. The $\zeta$ value is independent of the electrode potential as long as the potential falls within the range of the film formation (data not shown) and depends only on the bulk concentration of the wire. Figure 7 shows a linear dependence of $\theta$ on $t^{1/2}$, which confirms the diffusion-limited adsorption of **1** according to the Koryta equation (5). Such adsorption transients should be sensitive to the state of the wire **1** in the bulk of the solution and on the electrode surface. To see the effect of αCD on the compact film formation of **1** the adsorption transients at different αCD concentrations were recorded for $5 \times 10^{-6}$ M wire **1** in 0.1 M KF and 20% ethanol/water solvent. One of these transients is also shown in Fig. 7 (full circles) for $1.7 \times 10^{-3}$ M αCD addition. The characteristic time $\zeta$ of the compact film formation of the wire **1** decreases to $\zeta = 28$ s and the response remains linear confirming the diffusion-controlled process also in

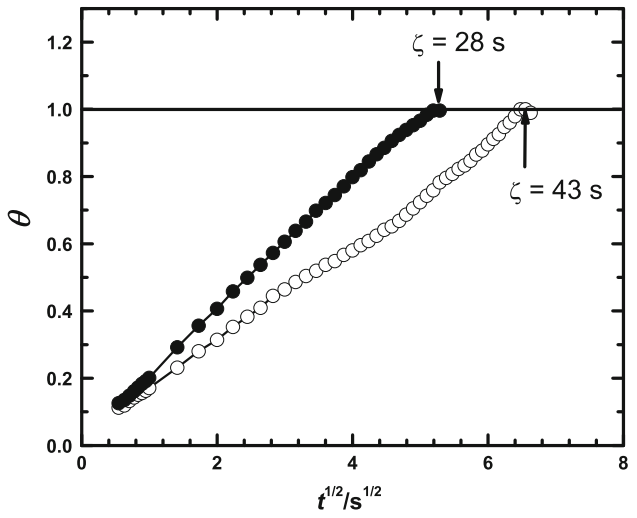


**Fig. 7** Time dependence of the electrode surface coverage $\theta$ for $5 \times 10^{-6}$ M wire **1** in the absence (*open circles*) and presence (*filled circles*) of $1.7 \times 10^{-3}$ M αCD in the 20% ethanol/water solution of 0.1 M KF obtained on HMDE at potential −0.6 V, at frequency 160 Hz and amplitude 5 mV

the presence of αCD in the solution bulk. The value of differential capacitance of the compact film **1** changes insignificantly on αCD addition. It is close to the capacitance value of the wire **1** in the absence of αCD and much higher than $C(t)$ of the monolayer formed solely by αCD molecules.

The overall dependence of ζ on the αCD concentration is shown in Fig. 8. At high αCD concentrations ζ reaches a limiting value giving another supporting evidence for the complex formation between **1** and αCD in the bulk of the

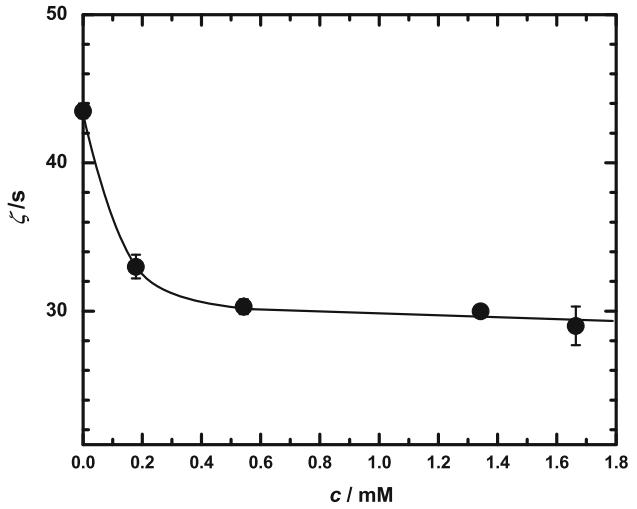


**Fig. 8** The characteristic time ζ required for a complete coverage of the HMDE by the wire **1** in 0.1 M KF in 20% ethanol/water solution as a function of αCD concentration. The analytical concentration of **1** was $5 \times 10^{-6}$ M, potential −0.6 V, frequency 160 Hz and amplitude 5 mV

solution. At sufficiently high CD concentration most of the wire **1** is in the form of a complex. Since the total concentration of the wire **1** stays constant the characteristic time ζ should depend only on the ratio $\Gamma^2/D_{eff}$ (see Eq. 5). The effective diffusion coefficient $D_{eff}$ is defined according to [21, 41] as $(D_w + D_c K_a[CD])/(1 + K_a[CD])$, where $D_w$ is the diffusion coefficient of the free wire **1**, $D_c$ is the diffusion coefficient of the complex, $K_a$ and [CD] have the same meaning as in the Eq. 3. A simple calculation assuming $K_a = 20$ mM$^{-1}$ and $D_c = 0.79\ D_w = 5 \times 10^{-7}$ cm$^2$/s shows that the effective diffusion coefficient $D_{eff} = 0.81 \times 10^{-6}$ cm$^2$/s differs only slightly from $D_w = 1 \times 10^{-6}$ cm$^2$/s. Therefore, the difference in ζ values is mainly due to the different surface concentration Γ of the wire in the compact film. This is an indirect but very important confirmation that the wire is adsorbed at the electrode/electrolyte interface in the form of the complex.

## Conclusions

The molecular wire **1** forms two types of the inclusion complexes with αCD in the aqueous environment containing 20% of ethanol, whereas βCD and γCD do not form such complexes with **1**. UV–Vis and fluorescence spectroscopic measurements proved the formation of 1:1 and 2:1 complexes of αCD with **1**. The $K_a$ values for both types of the complexes were obtained from the Benesi–Hildebrand type of analysis of the fluorescence emission spectra. For the [αCD–**1**] complex formation $K_a = 25 \pm 3$ mM$^{-1}$ in 20% v/v ethanol/water solvent, whereas for the [$(\alpha CD)_2$–**1**] complex it is only $K_a = 0.21 \pm 0.07$ mM$^{-2}$. The molecular wire **1** adsorbs on the electrode/electrolyte interface in a form of a compact film. If the bulk of the solution contains also the inclusion complex the time-dependent differential capacitance measurements are able to confirm the adsorption of **1** in the form of an inclusion complex. Such measurements represent an alternative electrochemical method for the confirmation of the complex formation and the adsorption abilities of such complexes based on a different molecular foot-print of the guest and its inclusion complex. The shortest extended viologen dication **1** serves as a model system and these findings will be used in our subsequent studies of the higher oligomers of the extended viologens. The final aim of these studies is to find the most suitable CD cavity that would both separate individual molecular wires from each other in the compact monolayer (mutually non-communicating wires) and possibly alter their electric conductivity properties (insulated wires). We suppose that the described insulation method will eliminate the cross-talk of wires [42] during the electric conductivity measurements of single molecules between two electrodes.

**Acknowledgments** This work was supported by Ministry of Education of the Czech Republic (MEB041006, LC510 and COST D36 OC140) and by Grant Agency of the Czech Republic GACR (203/08/1157, 203/09/1607) and Grant Agency of the Academy of Sciences GAAV (IAA400400802).

## References

1. Szejtli, J.: Introduction and general overview of cyclodextrin chemistry. Chem. Rev. **98**, 1743–1753 (1998)
2. Saenger, W., Jacob, J., Gessler, K., Steiner, T., Hoffmann, D., Sanbe, H., Koizumi, K., Smith, S.M., Takaha, T.: Structures of the common cyclodextrins and their larger analogues—beyond the doughnut. Chem. Rev. **98**, 1787–1802 (1998)
3. Szejtli, J.: Cyclodextrins and Their Inclusion Compounds. Akademiai Kiado, Budapest (1982)
4. Li, S., Purdy, W.C.: Cyclodextrins and their applications in analytical chemistry. Chem. Rev. **92**, 1457–1470 (1992)
5. Funston, A., Kirby, J.P., Miller, J.R., Pospíšil, L., Fiedler, J., Hromadová, M., Gál, M., Pecka, J., Valášek, M., Zawada, Z., Rempala, P., Michl, J.: One-electron reduction of an "extended viologen" *p*-phenylene-bis-4,4′-(1-aryl-2,6-diphenylpyridinium) dication. J. Phys. Chem. A **109**, 10862–10869 (2005)
6. Valášek, M., Pecka, J., Jindřich, J., Calleja, G., Craig, P.R., Michl, J.: Oligomers of "extended viologen", *p*-phenylene-bis-4,4′-(1-aryl-2,6-diphenylpyridinium), as candidates for electron-dopable molecular wires. J. Org. Chem. **70**, 405–412 (2005)
7. Pospíšil, L., Fiedler, J., Hromadová, M., Gál, M., Valášek, M., Pecka, J., Michl, J.: Search for a one-electron reduction of the cation radical of an "extended viologen" *p*-phenylene-bis-4,4′-(1-aryl-2,6-diphenylpyridinium). J. Electrochem. Soc. **153**, E179–E183 (2006)
8. Taniguchi, M., Kawai, T.: Effect of α-cyclodextrin coating on electronic properties of molecular wires. Chem. Phys. Lett. **431**, 127–131 (2006)
9. Cacialli, F., Wilson, J.S., Michels, J.J., Daniel, C., Silva, C., Friend, R.H., Severin, N., Samorì, P., Rabe, J.P., O'Connell, M.J., Taylor, P.N., Anderson, H.L.: Cyclodextrin-threaded conjugated polyrotaxanes as insulated molecular wires with reduced interstrand interactions. Nat. Mater. **1**, 160–164 (2002)
10. Frampton, M.J., Anderson, H.L.: Insulated molecular wires. Angew. Chem. Int. Ed. **46**, 1028–1064 (2007)
11. Shimomura, T., Akai, T., Fujimori, M., Heike, S., Hashizume, T., Ito, K.: Conductivity measurement of insulated molecular wire formed by molecular nanotube and polyaniline. Synth. Met. **153**, 497–500 (2005)
12. Shimomura, T., Akai, T., Abe, T., Ito, K.: Atomic force microscopy observation of insulated molecular wire formed by conducting polymer and molecular nanotube. J. Chem. Phys. **116**, 1753–1756 (2002)
13. Yoshida, K., Shimomura, T., Ito, K., Hayakawa, R.: Inclusion complex formation of cyclodextrin and polyaniline. Langmuir **15**, 910–913 (1999)
14. Muñoz de la Peña, A., Salinas, F., Gómez, M.J., Acedo, M.I., Sánchez Peña, M.: Absorptiometric and spectrofluorimetric study of the inclusion complexes of 2-naphthyloxyacetic acid and 1-naphthylacetic acid with β-cyclodextrin in aqueous solution. J. Incl. Phenom. Mol. Recognit. Chem. **15**, 131–143 (1993)
15. Schneider, H.J., Hacket, F., Volker, R., Ikeda, H.: NMR studies of cyclodextrins and cyclodextrin complexes. Chem. Rev. **98**, 1755–1785 (1998)
16. Das, P., Chakrabarty, A., Haldar, B., Mallick, A., Chattopadhyay, N.: Effect of cyclodextrin nanocavity confinement on the photophysics of a β-carboline analogue: a spectroscopic study. J. Phys. Chem. B **111**, 7401–7408 (2007)
17. Paul, B.K., Samanta, A., Guchhait, N.: Modulation of excited-state intramolecular proton transfer reaction of 1-hydroxy-2-naphthaldehyde in different supramolecular assemblies. Langmuir **26**, 3214–3224 (2010)
18. Pospíšil, L., Hromadová, M., Gál, M., Bulíčková, J., Sokolová, R., Filippone, S., Yang, J., Guan, Z., Rassat, A., Zhang, Y.: Redox potentials and binding enhancement of fullerene and fullerene–cyclodextrin systems in water and dimethylsulfoxide. Carbon **48**, 153–162 (2010)
19. Matsue, T., Osa, T., Evans, D.H.: Determination of some physical constants of cyclodextrin complexes by electrochemical methods. J. Incl. Phenom. Mol. Recognit. Chem. **2**, 547–554 (1984)
20. Nuwer, M.J., O'Dea, J.J., Osteryoung, J.G.: Kinetics and thermodynamics of inclusion of *p*-nitrophenolate with α-cyclodextrin measured with pulse voltammetry. J. Phys. Chem. **95**, 10070–10076 (1991)
21. Taraszewska, J., Piasecki, A.K.: Inclusion complexes of isomeric chloronitrobenzenes with α- and β-cyclodextrins studied by polarography: analysis of the possibilities of the method. J. Electroanal. Chem. **226**, 137–146 (1987)
22. Strelets, V.V., Mamedjarova, I.A., Nefedova, M.N., Pysnograeva, N.I., Sokolov, V.I., Pospíšil, L., Hanzlík, J.: Electrochemistry of inclusion complexes of organometallics: complexation of ferrocene and azaferrocene by cyclodextrins. J. Electroanal. Chem. **310**, 179–186 (1991)
23. Goledzinowski, M.: The influence of α-, β- and γ-cyclodextrins on the kinetics of the electrode reactions in 1 M $NaClO_4$ and 0.5 M $Na_2SO_4$ aqueous solutions. J. Electroanal. Chem. **267**, 171–189 (1989)
24. Hromadová, M., de Levie, R.: A sodium-specific condensed film of α-cyclodextrin at the mercury | water interface. J. Electroanal. Chem. **465**, 51–62 (1999)
25. Hromadová, M., Pospíšil, L., Záliš, S., Fanelli, N.: Electrochemical detection of host–guest interactions of dicarboximide pesticides with cyclodextrins. J. Incl. Phenom. Macrocycl. Chem. **44**, 373–380 (2002)
26. Yasuda, A., Kondo, H., Itabashi, M., Seto, J.: Structure changes of viologen + β-cyclodextrin inclusion complex corresponding to the redox state of viologen. J. Electroanal. Chem. **210**, 265–275 (1986)
27. Sivagnanam, U., Palaniandavar, M.: Selective inclusion of methylviologen by β-cyclodextrin: effect of cyclodextrins on the electrochemistry of methylviologen. J. Electroanal. Chem. **341**, 197–207 (1992)
28. Mirzoian, A., Kaifer, A.E.: Reactive pseudorotaxanes: inclusion complexation of reduced viologens by the hosts β-cyclodextrin and heptakis(2,6-di-O-methyl)-β-cyclodextrin. Chem. Eur. J. **3**, 1052–1058 (1997)
29. Kitamura, F., Ohsaka, T., Tokuda, K.: Effect of complexation by cyclodextrins on the voltammetric characteristic of viologens adsorbed on an HMDE. J. Electroanal. Chem. **368**, 281–284 (1994)
30. Lee, C.M., Moon, M.S., Park, J.W.: Spectroelectrochemical study on monomer/dimer equilibria of methylalkylviologen cation radicals with and without α-cyclodextrin. J. Electroanal. Chem. **407**, 161–167 (1996)
31. Lee, C.M., Sung, Y.W., Park, J.W.: Dependence of dimerization of electrogenerated methylalkylviologen radical cations on the length of alkyl chain in the presence of γ-cyclodextrin. J. Electroanal. Chem. **431**, 133–139 (1997)
32. Yasuda, A., Seto, J.: Electrochemical behaviour of viologen-cyclodextrin inclusion complexes. The case of non-alkyl group substituted viologen. J. Appl. Electrochem. **18**, 333–338 (1988)

33. Gattuso, G., Gargiulli, C., Parisi, M.F.: Threading cyclodextrins in chloroform: a [2]pseudorotaxane. Int. J. Mol. Sci. **8**, 1052–1063 (2007)
34. Park, J.W., Song, H.E., Lee, S.Y.: Face selectivity of inclusion complexation of viologens with $\beta$-cyclodextrin and 6-O-(2-sulfonato-6-naphthyl)-$\beta$-cyclodextrin. J. Phys. Chem. B **106**, 7186–7192 (2002)
35. Yan, J., Dong, S., Li, J., Chen, W.: Formation of self-assembled monolayers on gold electrodes with inclusion complexes of cyclodextrins and viologens. J. Electrochem. Soc. **144**, 3858–3865 (1997)
36. Valášek, M., Betík, R., Pecka, J., Michl, J.: J. Org. Chem. (submitted)
37. Benesi, H.A., Hildebrand, J.H.: A spectrophotometric investigation of the interaction of iodine with aromatic hydrocarbons. J. Am. Chem. Soc. **71**, 2703–2707 (1949)
38. Chen, M., Diao, G., Zhang, E.: Study of inclusion complex of $\beta$-cyclodextrin and nitrobenzene. Chemosphere **63**, 522–529 (2006)
39. Saha, A., Nayak, S.K., Chattopadhyay, S., Mukherjee, A.K.: Study of charge transfer interactions of a resorcin[4]arene with [60]- and [70]fullerenes by the absorption spectrometric method. J. Phys. Chem. A **108**, 8223–8228 (2004)
40. Heyrovský, J., Kůta, J.: Základy Polarografie. Nakladatelství Československé Akademie Věd, Praha (1962)
41. Taraszewska, J.: Complexes of $\beta$-cyclodextrin with chloronitrobenzenes and with solvents in water + organic solvent mixtures. J. Incl. Phenom. Macrocycl. Chem. **10**, 69–78 (1991)
42. Pospíšil, L., Hromadová, M., Gál, M., Valášek, M., Fanelli, N., Kolivoška, V.: Irregular polarographic currents obey Feigenbaum universality route from order to chaos. Collect. Czechoslov. Chem. Commun. **74**, 1559–1570 (2009)